Available online at www.elixirpublishers.com (Elixir International Journal)

Thermal Engineering

Elixir Thermal Engg. 176 (2023) 56724-56731

ISSN: 2229-712X

Modeling of a Multifunction Family Kiln Prototype for Biochar Production and Energy Valorization

Moussa dit Corneille Tarpilga[1], GaëlLassina Sawadogo[2], Bétaboalé Naon[3]and François Ouedraogo[4]

[1,3,4]Laboratory of Materials and Environment (LAME), Nazi Boni University, 01 BP 1091 BoboDioulasso, Burkina Faso.

[2]Laboratory of Renewable Thermal Energies (LETRE), Nazi Boni University, 01 BP 1091 BoboDioulasso, Burkina Faso

ARTICLE INFO

Article history:

Received:13 January 2023;

Received in revised form:

15 March 2023;

Accepted: 25 March 2023;

Keywords

Multifunction Family Furnace,

Biochar,

Alternative Energy,

Modeling.

ABSTRACT

Excessive wood consumption in Burkina Faso has led not only to deforestation, but also to soil degradation. The preservation of ecosystem balances, the management of soil fertility and the safeguarding of forests are major issues for future generations. It is in this context that our work has focused on the development of an energy conversion technology that effectively uses little-used agricultural residues (cotton stalks, bare corn cobs, rice husks, etc.). This device is a multifunction family furnace that produces biochar for soil amendment and provides alternative energy for household needs. The physical and mathematical modeling of the oven based on the nodal method whose equations were solved by implicit finite differences allowed to describe its thermal behavior. K-type thermocouples were used for the experimental study to validate the mathematical model. Indeed, the pyrolysis temperature of the bare corn cobs is on average 450 °C. The model allowed us to show that the thickness of the pyrolysis chamber influences the pyrolysis temperature and reduces the pyrolysis time. For a thickness of 8 cm of the pyrolysis chamber, the average pyrolysis time is 1 hour 30 minutes. The study also showed that the variation of the ambient temperature does not influence the pyrolysis temperature. Moreover, the thickness of the insulation chamber affects the external wall temperature but not the pyrolysis temperature.

1. Introduction

Burkina Faso is a landlocked Sahelian country in West Africa. Most of its population, 85%, lives from agriculture [1]. For some time, the country has been experiencing increased degradation of its natural resources, particularly the soil, which has reduced the yield of agricultural production [2]. By soil degradation, we mean the loss of its potential, especially the depletion of soil nutrients [3]. Indeed, this soil degradation is caused on the one hand by the effects of climate change and on the other hand by poor farming practices, which have resulted in desertification and the continued decline in soil fertility [4]-[6]. The significant decline in agricultural yields is noted among producers. To obtain good yields, farmers resort to chemical fertilizers as an amendment [6]. However, it is necessary to recognize the drifts noted in the use of fertilizers by the farmers, i.e. the non-respect of the doses and the always late contributions [6]. This results in the ineffectiveness of these fertilizers which constitutes a loss of money and is a source of environmental pollution [7], [8].

In addition, farmers use compost to amend the soil, but it is washed away after the first rains. Farmers have little-used agricultural residues such as cotton stalks, maize stalks, rice husks, etc. These residues are burned at the beginning of the rainy season for new sowing. These residues are burned at the beginning of the rainy season for new planting. The valorization of these residues can contribute in a decisive way to ensure the maintenance of the fertility of cultivable soils [9]. They can also be used for the production of biochar. In recent decades, biochar has attracted increasing interest for agricultural and environmental applications [10]. In fact, when used as a soil amendment, biochar, serves for carbon sequestration [11], improves the physical properties of the soil [10], increases the water holding capacity [12], and acts as an absorbent for pollutants and nutrients [13]. Biochar can be produced by thermochemical decomposition of biomass at temperatures of 200-900 °C in the presence of little or no oxygen, which is commonly referred to as pyrolysis [14]. Pyrolysis is generally fast, intermediate, or slow depending on residence time and temperature. Slow and intermediate pyrolysis processes with a residence time of a few minutes to several hours or days are generally preferred for biochar production [15]. However, its production remains an important issue for its popularization in the southern countries and a global issue for the environment. There are several industrial or artisanal devices that allow the production of biochar [16] [17], [18], [19] [20].

Recent artisanal technologies of pyrolysis valorizing biomasses exist but the scientific description of the pyrolysis process in these equipment's not yet well established. It is therefore necessary to make a scientific approach on the production technique that provides the production of optimal biochar while reducing the rate of emission of greenhouse gases (GHG) and also contribute to the fight against deforestation.

It is in this context that this work is part of the numerical modeling of a device capable of producing biochar and valorizing the energy provided during pyrolysis for cooking. It is an energy conversion technology that aims to effectively use agricultural residues poorly valued in order to reduce the abusive cutting of wood and restore cultivable soils through the biochar produced.

2. Materials

2.1. Thermocouples

Type K thermocouples were installed at several locations in the furnace to measure temperatures during pyrolysis (Figure 1). The extension cable is made of ceramic fiber wires that can withstand continuous temperature up to over 1000 °C.

Figure 1: Type K thermocouple

2.2. Bare corn cobs

Bare corn cobs are agricultural residues that are poorly valorized after the harvest (Figure 2). The characteristics of corn cobs are satisfactory for combustion as well as for pyrolysis [21].

Figure 2:Bare corn cobs

3. Method

3.1. Physical model of the device

The new appliance is a multifunction family furnace consisting of three chambers (combustion chamber, pyrolysis chamber and insulation chamber), a firebox to accommodate the pot, and a base on which the entire oven sits (Figure 3).

- The combustion chamber: it is located in the center of the oven from where the combustion takes place.

- The pyrolysis chamber: it is the compartment that receives the biomass to be pyrolyzed.

- The isolation chamber: it is a hermetically sealed chamber located outside the pyrolysis chamber.

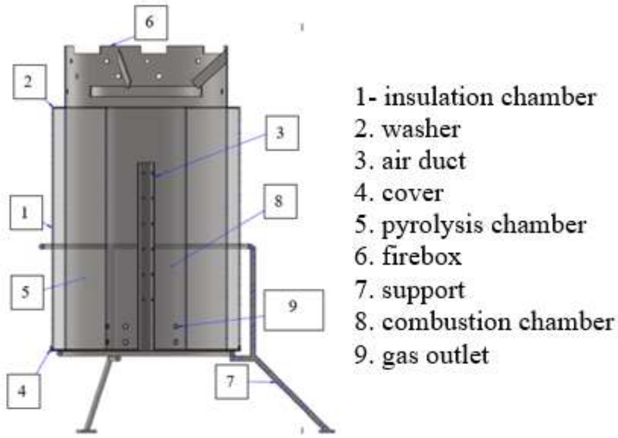

Figure 3: Description of the multifunction family furnace

3.2. Development of the prototype

Based on the previously described physical model, a prototype was designed (Figure 4).

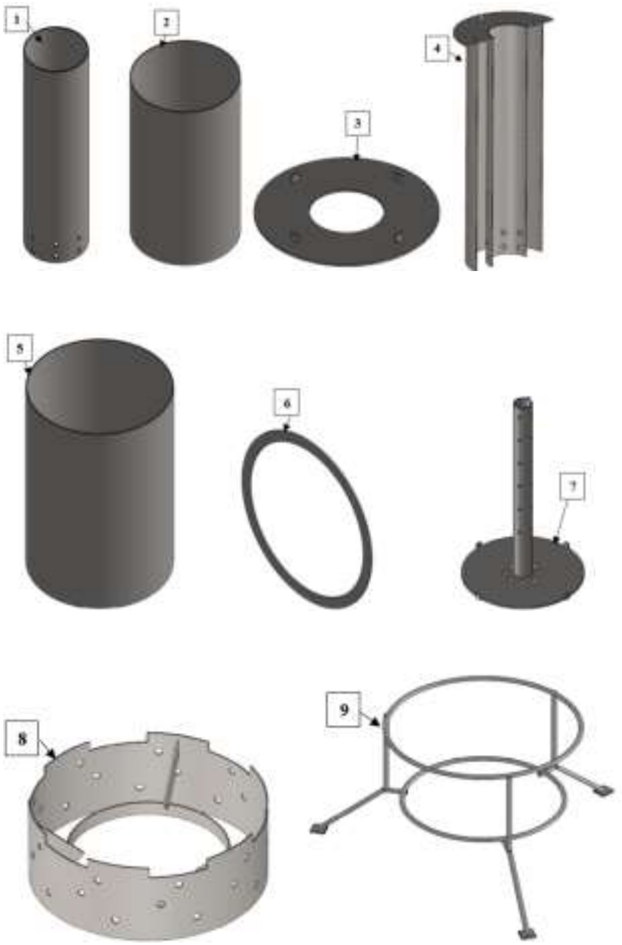

1- Washer 2 for closing the isolation chamber

2- Air duct connected to the furnace cover

3- Oven firebox

4- Oven support

5- **Inner cylindrical sheath**

6- **Outer cylindrical sleeve**

7- **Upper base washer 1**

8- **Formation of combustion and pyrolysis chambers**

9- **Metal barrel**

Figure 4: Development of the multifunction family kiln
Different Modes of Heat Transfer

Multifunction family furnace uses the agricultural residues poorly valorized such as bare corn cobs, cotton stalks, rice husks, etc. The pyrolysis chamber is first loaded with the biomass to be pyrolyzed and then closed with the lid. Then the combustion chamber is loaded with the fuel to be burned and ignited. Finally, the fuel is ignited from the top of the furnace and the combustion front is from top to bottom. Heat is transferred from the inside to the outside by conduction, convection and radiation (figure 5).

Combustion initiates pyrolysis from which we witness three modes of heat transfer:

- heat transfer by conduction: between the walls and the biomass, in the pyrolysis chamber;
- heat transfers by radiation: wall-biomass and to the outside environment;
- heat transfers by convection: in the combustion chamber, in the insulation chamber and with the outside environment.

At the end of the pyrolysis, we obtain biochar (figure 6) in the pyrolysis chamber.

Figure 5 shows the different modes of heat transfer that take place during the operation of the multifunction family furnace.

In this study, we did not consider the phase change, although it is important in the drying of moisture-containing biomass prior to pyrolysis.

3.3. Mathematical model

3.3.1. Simplifying assumptions

A model taking into account the most justifying phenomena is proposed. This model is based on the following simplifying assumptions:

- thethermophysical properties of the materials are assumed to be constant;
- at the initial time, the temperature is the same on the walls and in the chambers for a given level of the furnace;
- the speed and the temperature of the air are constant in the surrounding environment;
- the radiation outside, i.e., in the surrounding environment, is neglected.

3.3.2. Setting in equations

The mathematical model used in our study is based on the nodal method. In fact, in the case of static thermal systems, the equations governing the heat transfers can be established using this method [22]. It is based on an analogy between thermal/electrical heat transfers and is particularly adapted to problems of analysis of complex systems involving different fields of physics [23]. In general, modeling a system based on the nodal method amounts to setting up a network of thermal capacitances($C_i = \rho_i c_i V_i$),or heat sinks and thermal resistances. By applying Kirchhoff's law to the network of heat capacities and heat resistances schematizing the different modes of heat transfer in a considered physical model element, the general heat balance equation can be obtained [24].

$$m_i C_{pi} \frac{\partial T_i}{\partial t} = \sum_{i \neq j} d_{i,j}(T_i - T_j) + \sum_i Q_i \qquad (1)$$

with:

m_i: **Node mass** i **(Kg)**,
C_{pi}: **heat capacity at constant pressure** $(J.Kg^{-1}.K^{-1})$
d_{ij}: **thermal conductance between nodes i et j** $(W.K^{-1})$
,Q_i: **heat source produced by the material i** (J)

- The conductance of the heat transfer mode imposed at the interval of a node, is noted as follows thus:
- **conductive conductance is** $d_{ij} = \frac{\lambda S}{e}$
- **convective conductance is** $d_{ij} = hS$
- **radiation conductance is**

$$d_{ij} = \varepsilon\sigma(T_i + T_j)(T_i^2 + T_j^2)$$

with:

λ: **thermal conductivity** $(w.m^{-1}.K^{-1})$
S: **surface crossed by the heat flow** (m^2)
e: **Characteristic thickness** (m)
h: **convection coefficient** (W)
ε: **Emissivity of the wall**
σ: **constant of Stefan Boltzmann** $(5,67.10^{-8}m^{-2}K^{-4})$

3.3.3. Heat transfer equations for the different components of the multifunction family oven

The thermophysical properties of the materials used in the equations are reported in Table 1.

Convection conditions are greatly influenced by external conditions, which often leads to discrepancies between theoretical and experimental studies [25]. In the characterization of heat transfer between any fluid and a wall, the Nusselt number (Nu) is used:

$$Nu = \frac{h_a L_c}{\lambda} \qquad (2)$$

With$h_a$the heat exchange coefficient, L_c the characteristic length and λ the thermal conductivity of the fluid:

$$L_c = \frac{4xS}{P} \qquad (3)$$

The Nusselt number is determined by empirical correlations depending on the type and regime of transfer. In the case of our study, the convection observed inside the isolation chamber is natural convection. We will therefore use the following relation [26].

$$Nu = C(G_r P_r)^m \qquad (4)$$

With G_r *and* P_r are the Grashof number and the Prandtl number, respectively. C and m are constants related to the value of the product $G_r P_r$.

$$G_r = \frac{\beta g \Delta T \rho^2 L_C{}^3}{\mu^2} \qquad (5)$$

$$P_r = \frac{C_p \mu}{\lambda} \qquad (6)$$

β is the cubic coefficient of expansion
βgΔT is therefore the modulus of the acceleration produced by the thermal expansion due to the variation ΔT of the temperature T_0.

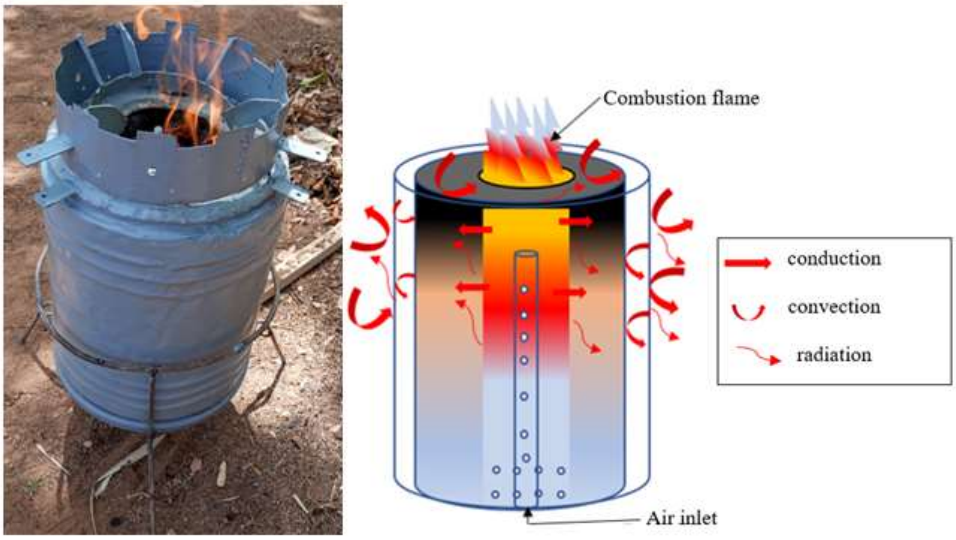

Figure 5: Different modes of heat transfer in a multifunction family furnace

Figure 6: Biochar produced after pyrolysis

Table 1: Thermophysical constants of the materials used

Designations	λ $W/(m.K)$	C_p $J/(Kg.K)$	ρ Kg/m^3
Iron sheet	70	478	7850
Bare corn cobs	0,093	1000	200
Air	0,025	1005	

Table 2: transfer coefficients by Natural convection valid for all fluids

Geometry	G_rP_r	C	m
Vertical plate and cylinder	$10^4 - 10^9$	0,59	1/4
	$10^9 - 10^{13}$	0,021	2/5

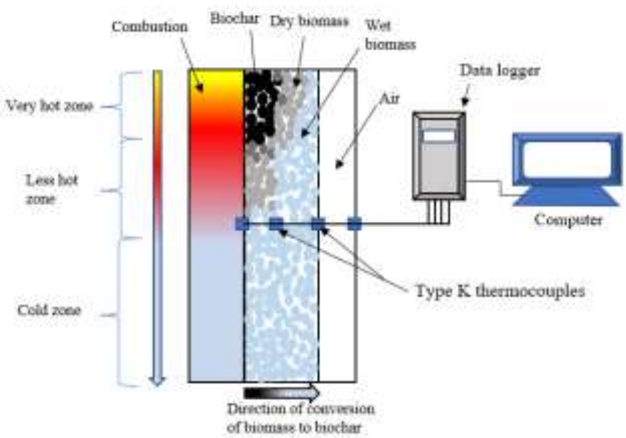

Figure 7: Experimental study of pyrolysis

The correlation for the calculation of transfer coefficients by Natural convection valid for all fluids as in the case of our study is noted in the following table [26].

The external faces of the combustion chamber exchange heat by convection with the surrounding environment. As the air velocity is not negligible, we have chosen the Mc Adam correlation to determine the exchange coefficient ($\mathbf{h_a}$) of these faces [22]:

$$h_a = 5,7 + 3,8V_a \quad (7)$$

Speed of the air: $V_a = 3\ m/s$

Thermal conductivity: $\lambda = 0,00031847 \text{x} T\ en\ w/(m.K)$

Mass heat: $C_p = 0,9362 + 0,0002 \text{x} T\ en\ kJ/(kg.K)$

Dynamic viscosity:

$$\mu = 0,0447.10^{-5} \text{x} T^{0,7775}\ en\ kg/(m.s)$$

Density: $\rho = \frac{353}{T}\ en\ kg/m^3$

Enthalpy: $h = 1,42\left(\frac{\Delta\theta}{L}\right)^{1/4}$

3.3.4. Boundary condition

At t= 0, the temperature of the different chambers and the walls is equal to the ambient temperature T_i= 39 °C. The temperature of the inner wall for the simulation is interpolated from the experimental temperature.

3.3.5. Algorithm for solving the system

At the initial time t_i, the temperatures of the walls as well as the chambers are initialized to the room temperature and the heat transfer coefficients (convective, radiative) are thus calculated. At t_i+Δt, where Δt is the time step, solving the system of algebraic equations leads to new values of the temperature of the components of the multifunction oven which are compared to arbitrary values. If the difference between these two temperatures is greater than the desired accuracy, the calculated temperature values replace the new arbitrary values and the procedure described above is repeated until convergence is achieved. The convergence is obtained when the criterion of the equation $\frac{T^{t+\Delta t} - T^t}{T^{t+\Delta t}} \leq 10^{-3}$ is satisfied.

3.4. Experimental study for the validation of the model

In order to validate the mathematical model presented above, it is therefore necessary to make a comparison between the numerical results and the experimental results. However, an experimental study was conducted on the new prototype (multifunction family furnace). In this case, we installed K-type thermocouples on each node described in the previous diagram (Figure 7). The experimental results will be compared to the numerical results for the validation of the model.

Bare corn cobswere used as fuel in the combustion chamber and as biomass to be pyrolyzed in the pyrolysis chamber. Before the start of combustion, the initial temperature in all locations was taken to 39 °C. The mass of rachis to be pyrolyzed is 3.4 kg and the biomass to be burned is 1 kg of rachis to be burned. A temperature data logger of model Comet_MS6D was used. The obtained data are processed and compiled in a computer.

4. Results and Discussion

Figure 8 shows the numerical and experimental temperature profiles that takes place in the pyrolysis chamber of the kiln during the pyrolysis of bare corn cobs.

Figure 8 has shown that the evolution over time of the pyrolysis temperature in the multifunction furnace obtained from our model was in good agreement (qualitative and quantitative) with that of the experimental study. Indeed, the maximum relative difference between our results and those obtained experimentally is about 9%. This discrepancy may result from the semi-empirical correlations we used for the calculation of the natural convection heat transfer coefficients and the assumptions made.

It should also be noted that at the end of the pyrolysis we smother the combustion chamber with sand, resulting in a rapid drop in the pyrolysis temperature. This also justifies the fact that the pyrolysis temperature curve is at the bottom of the numerical one.

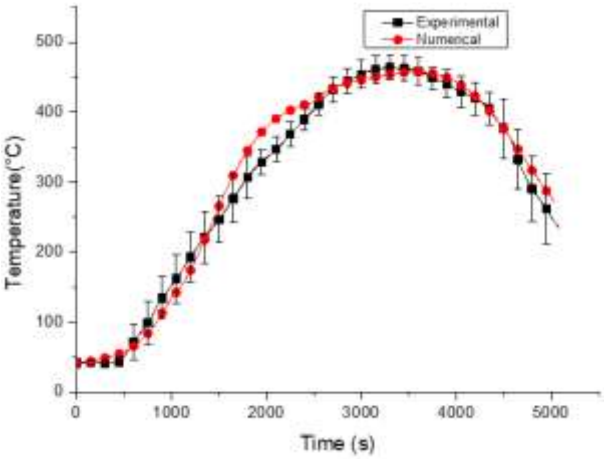

Figure 8: The numerical and experimental temperature profiles

This model can now be used to simulate the operation of the multifunction oven under different conditions. Thus, in addition to corn stover, we used cotton stalks and rice husk to improve the understanding of the operation of the kiln.

4.1. Pyrolysis temperature versus pyrolysis chamber thickness

Figure 9 is showing the temporal profile of pyrolysis temperatures of bare corn cobs. As a function of the thickness of the pyrolysis chamber, the curves show the same gaits. We found that as soon as the combustion was initiated, the temperature of the pyrolysis chamber evolved to a maximum temperature, and then it decreased abruptly due to the fact that the combustion is choked after 4000 s.

When the thickness of the pyrolysis chamber increased, the amount of biomass to be pyrolyzed also increased, inducing a longer heating time and lower pyrolysis temperatures. Indeed, considering that the pyrolysis temperature is 250 °C, for a thickness of 2 cm the pyrolysis temperature was reached after 1200s while for a thickness of 14 cm it starts from 2250s. The results obtained for the three (3) types of biomass are similar. These results show that the thickness of the pyrolysis chamber influences the pyrolysis temperature. The smaller the thickness of the pyrolysis chamber, the higher the pyrolysis temperature.

4.2. Influence of the thickness of the insulation chamber on pyrolysis

Figures 10 show the pyrolysis temperature profiles according to the different thicknesses of the isolation chamber.

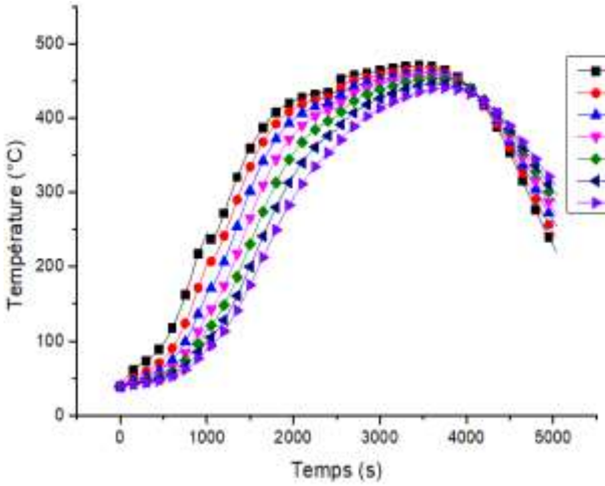

Figure 9: Time profile of pyrolysis temperature of corn cobs as a function of the thickness of the pyrolysis chamber

The temperature profiles of the pyrolysis chamber show almost the same trends independently of the thickness and the type of biomass. The results obtained show that the thickness of the insulation chamber does not influence the temperature of the pyrolysis chamber for temperatures lower than 400 °C. However, for temperatures higher than 400 °C, the increase of the thickness of the insulation chamber generates a small variation of the temperatures of the pyrolysis chamber. Indeed, the heat exchange coefficient by convection is function of the temperature and from 400°C the heat exchange coefficient by radiation is not negligible.

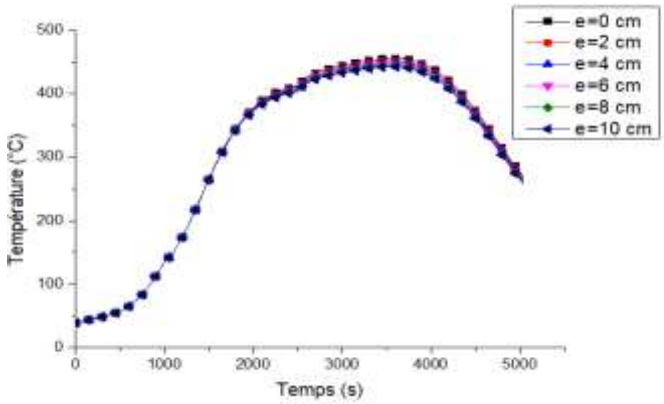

Figure 10: Time profiles of pyrolysis chamber temperatures as a function of insulation chamber thickness

4.3. Influence of the ambient air temperature on the pyrolysis

Figure 11 shows the pyrolysis temperature profiles when the ambient temperature varies.

The temperature profiles of the pyrolysis chamber show the same trends independently of the thickness and the type of biomass. However, a slight variation of the temperature profiles is observed at the beginning of the experiment. This variation is due to the initial conditions since at the beginning of the experiment, the oven temperature is in equilibrium with the ambient air temperature. These results show that the multifunction family oven can be used at any time of the year for pyrolysis, since the ambient temperature does not influence the pyrolysis of the biomass over time.

4.4. Influence of the thickness of the insulation chamber on the external wall temperatures of the furnace

The influence of the thickness of the insulation chamber on the external parietal temperatures of the furnace are presented in figure 12.

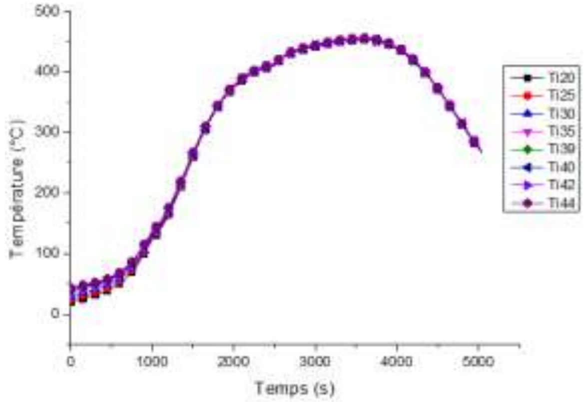

Figure 11: Temporal profile of the pyrolysis temperature according to the variation of ambient temperature (Ti)

Temperature profiles of the pyrolysis chamber show the same patterns independently of the thicknesses and the type of biomass. At the beginning of the experiment, the temperatures are confused and evolve very little. Indeed, the effusivity of the biomass being low, it delays the transmission of the heat from the inside (combustion chamber) to the outside (external wall of the furnace). Around 1500s, the external wall temperatures grow differently. This observed difference is due to the increase of the thickness of the insulation chamber which increases the exchange surface of the external wall of the furnace with the outside environment. Indeed, when the thickness increases, the external wall temperatures drop. In the absence of the insulation chamber, the external wall temperature of the furnace is 330°C, whereas with a 14cm thick insulation chamber the maximum temperature reached is 230°C. With 14cm of insulation the temperature difference is 100°C, however, the external wall temperature is still much higher than the one recommended in the standards (60°C).

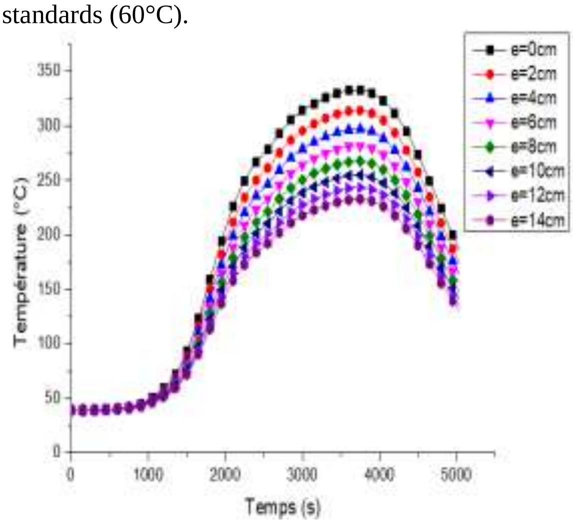

Figure 12: Temporal profiles of furnace external parietal temperature as a function of insulation chamber thickness.

5. Conclusion

In this paper, we have performed a numerical modeling and simulation of heat transfers in a multifunction family furnace. The methodology used is the nodal method and the equations governing the transfers in the oven were obtained by making an energy balance on each node by analogy between electrical and thermal transfers. The obtained equations were discretized by an implicit finite difference scheme and then solved by the Gauss algorithm. The mathematical model was then validated by comparing numerical and experimental results. The numerical results obtained allowed to understand the thermophysical mechanisms that take place in the pyrolysis chamber during the operation of the furnace. These obtained results show that the multifunction family oven pyrolyzes well the different biomasses used. In addition, these results show that the thickness of the chamber has little influence on the temperature of the pyrolysis chamber. The results obtained on the external walls induce that the air is not a good insulator for our system because it does not reduce the energy losses of the pyrolysis chamber. The results also show that the operation of the developed prototype is not influenced by the variation of the ambient temperature during the year.

References

[1] B. M. Pouya et al, "Farmer perceptions of technological options for integrated soil fertility management under sorghum and cowpea crops in the eastern region of Burkina Faso," Vol. 32, no. 1, p. 11, 2021.

[2] B. M. Pouya et al, "Socioeconomic determinants of soil degradation and adoption of soil fertility management technologies according to farmers' perceptions in the cotton-growing areas of burkinafaso," p. 10, June 2020.

[3] C.Reij, Traditional techniques for water and soil conservation in Africa. KARTHALA Editions, 1996.

[4] B. Bacye, H.S. Kambire, and A.S. Some, "Effects of farmers' fertilization practices on the chemical characteristics of a leached tropical ferruginous soil in the cotton zone of western Burkina Faso," International Journal of Biological and Chemical Sciences, vol. 13, no. 6, Art. no. 6, 2019, doi: 10.4314/ijbcs.v13i6.39.

[5] L.B.Tingueri, V.Bougouma-Yameogo, and M. Blanchard, "Assessing the sustainability of non-standard organic manure management practices in western Burkina Faso," 2019.

[6] A. Traoré, I. A. N. DA, K. TRAORE, P. BAZONGO, O. Traoré, and L. P. Yameogo, "Effect of the unique fertilizer formula 23-10-05 +3,6S+2,6Mg+0,3Zn on Barka maize yield in the South Sudan zone of Burkina Faso", Afrique SCIENCE, p. 11, 2020.

[7] S.Savci, "An agricultural pollutant: chemical fertilizer," International Journal of Environmental Science and Development, vol. 3, no. 1, p. 73, 2012.

[8] S.Czarnecki and R.-A.Düring, "Influence of long-term mineral fertilization on metal contents and properties of soil samples taken from different locations in Hesse, Germany," Soil, vol. 1, no. 1, pp. 23-33, 2015.

[9] B. Koulibaly, O. Traoré, D. Dakuo, P. N. Zombré, and D. Bondé, "Effects of crop residue management on yields and crop balances of a cotton-corn-sorghum rotation in Burkina Faso," TROPICULTURA, p. 7, March 2010.

[10] F. Masís-Meléndez, D. Segura-Chavarría, C. A. García-González, J. Quesada-Kimsey, and K. Villagra-Mendoza, "Variability of Physical and Chemical Properties of TLUD Stove Derived Biochars," Applied Sciences, vol. 10, no. 2, Art. no. 2, Jan. 2020, doi: 10.3390/app10020507.

[11] K.A. Spokas et al, "Biochar: a synthesis of its agronomic impact beyond carbon sequestration," Journal of environmental quality, vol. 41, no. 4, pp. 973-989, 2012.

[12] K.Karhu, T.Mattila, I.Bergström, and K.Regina, "Biochar addition to agricultural soil increased CH4 uptake and water holding capacity-Results from a short-term pilot field study," Agriculture, ecosystems & environment, vol. 140, no. 1-2, pp. 309-313, 2011.

[13] M.Ahmad et al, "Biochar as a sorbent for contaminant management in soil and water: a review," Chemosphere, vol. 99, pp. 19-33, 2014.

[14] A.Demirbas and G. Arin, "An overview of biomass pyrolysis," Energy sources, vol. 24, no. 5, pp. 471-482, 2002.

[15] R.Brown, "Biochar production technology," in Biochar for environmental management, Routledge, 2012, pp. 159-178.

[16] S.A.O. Lebongo, "Biochar production from rice husk: from the study of the resource to the valorization of the product", 2iE, Dissertation for the obtaining of the specialized masters in electrical engineering, energy and renewable energies (GEER), Sept. 2011. Accessed on: 18 August 2021.[Online]. Available at:
http://www.secheresse.info/spip.php? article56589.

[16] S. A. O. Lebongo, "Production of biochar from rice husk: from the study of the resource to the valorization of the product", 2iE, Dissertation for the obtaining of the masters specialized in electrical engineering, energy and renewable energies (GEER), Sept. 2011. Accessed on: 18 August 2021.[Online]. Available from:
http://www.secheresse.info/spip.php?article56589

[17] H.P. Schmidt, P. Taylor, A. Eglise, and C. Arbaz, "Kon-Tiki flame curtain pyrolysis for the democratization of biochar production," Biochar J, vol. 1, p. 14-24, 2014.

[18] N.R. Pandit, J. Mulder, S. E. Hale, H. P. Schmidt, and G. Cornelissen, "Biochar from "KonTiki" flame curtain and other kilns: Effects of nutrient enrichment and kiln type on crop yield and soil chemistry," PLOS ONE, vol. 12, no. 4, p. e0176378, Apr. 2017, doi: 10.1371/journal.pone.0176378.

[19] M.Njenga et al, "Gasifier as a cleaner cooking system in rural Kenya," Journal of Cleaner Production, vol. 121, pp. 208-217, May 2016, doi: 10.1016/j.jclepro.2016.01.039.

[20] I.G.Harouna et al, "Determination of processes suitable for cotton stalk carbonization and torrefaction by partial combustion using a metal kiln," Energy for Sustainable Development, vol. 24, p. 50-57, 2015.

[21]D.Ouédraogo, "Modeling heat transfer in a pressure cooker: Application to the development of energy efficient equipment for the food service sector," 2020.

[22] G.L.Sawadogo, "Modeling heat transfer phenomena in an insulated oven with local materials: Application to the energy optimization of meat grilling equipment," thesis, Josep Ki Zrebo University, Ouagadougou, 2020.

[23] J.B.Saulnier and A. Alexandre, "Thermal modeling by the nodal method: its principles, successes, and limiting doses," Rev. Gen. Therm, vol. 24, no. 280, pp. 363-372, 1985.

[24] A.Compaore, "Etude des performances thermiques d'un habitat type du Burkina Faso. Application : Contribution à la mise en place d'une règlementation thermique ", PhDthesis, University of Ouaga I Pr Joseph KI ZERBO, 2018.

[25]C.Garnier, "Numerical modeling of open natural convection flows within an asymmetrically heated vertical channel," PhD Thesis, Université Pierre et Marie Curie, 2014.

[26]Y.Jannot, Heat transfers. 2012. [Online]. Available from:
http://www.edilivre.com/transferts-thermiques-cours-et-55-exercices-corrig 20c28f73fc.html#.VyIS3nqHhPI.

Special thanks

This work was carried out within the framework of the BIOPROTECHSOL project carried out at the Nazi Boni University (UNB). They were financed entirely by the Academy of Research and Higher Education (ARES) of the Kingdom of Belgium